Structural properties of $Si_{1-x}Ge_x$ alloys: A Monte Carlo simulation with the Stillinger-Weber potential

Mohamed Laradji and D. P. Landau
Center for Simulational Physics, The University of Georgia, Athens, Georgia 30602

B. Dünweg
Center for Simulational Physics, The University of Georgia, Athens, Georgia 30602
and Institut für Physik, Johannes Gutenberg-Universität, Postfach 3980, D-55099 Mainz, Germany
(Received 6 September 1994; revised manuscript received 21 November 1994)

The structural properties of binary silicon-germanium alloys are investigated by means of large-scale constant-pressure Monte Carlo simulations of the Stillinger-Weber model. At low temperatures, the binary-mixture phase separates into Si-rich and Ge-rich phases. The two-phase coexistence region is terminated by a critical point that belongs to the mean-field universality class. We also studied the structural properties of pure Si and Ge as well as the binary mixture. In particular, we found that the linear thermal expansions for both Si and Ge are in agreement with experiments, and that Végard's law is valid at temperatures above the critical point. Finally, we compare the bond-length and bond-angle distributions with earlier analytical and numerical calculations based on the Kirkwood potential.

I. INTRODUCTION

Semiconductor alloys, which are solid solutions of two or more semiconducting elements, have important technological applications, especially in the manufacture of electronic and electro-optical devices.[1] For this reason, $Si_{1-x}Ge_x$ alloys have received extensive attention, as reflected by the recent experimental, theoretical, and numerical studies. Among the many unsolved questions concerning these alloys is their bulk phase behavior. Although it is well known that $Si_{1-x}Ge_x$ alloys are mixed at room and higher temperatures, the presence and the locus of an unmixing phase transition at low temperatures remains an open question due to the lack of experimental evidence.

In contrast to some metallic alloys, $Si_{1-x}Ge_x$ cannot be adequately modeled by simple lattice-gas Ising-like models, due to the important contribution of bond elasticity to the total energy. As a result, more refined models which take this effect into account must be considered. Empirical models have been proposed, some of which are based on small perturbations of the site positions around their ground-state values in the diamond lattice, such as the Kirkwood model[2] and the Keating model.[3] Other models are constructed in such a way that they predict the diamond-lattice structure at low temperatures and a melted liquid structure at high temperatures. These correspond, for instance, to the Stillinger-Weber potential,[4] the Biswas-Hamman potential,[5] and the Tersoff potential.[6] Cowley[7] has made a comparative study of the predicted lattice dynamics of the last three models with experimental data, and showed that the Stillinger-Weber (SW) model, which ironically is the simplest one, gives the best overall comparison.

Traditionally, studies of surface and bulk properties of semiconductors are performed via molecular-dynamics methods.[4,8,9] However, these methods use very small time scales and are, in general, performed in the microcanonical or the canonical ensemble where the compositions of the two elements are fixed throughout the whole simulation. Consequently the Monte Carlo (MC) method remains the most powerful tool for studying $Si_{1-x}Ge_x$ phase behavior. In this paper, we present our recent results for a detailed constant pressure MC simulation of the SW potential in the semi-grand-canonical[10] ensemble combined with a finite-size scaling analysis.

There are already studies of $Si_{1-x}Ge_x$ phase behavior in the literature. Kelires and Tersoff[11] performed a constant-pressure MC simulation of the Tersoff potential in the semi-grand-canonical ensemble. They showed that Si and Ge phase separate below a critical temperature located around 170 K. Their simulation was, however, performed on only small system sizes, and no finite-size analysis was made. Later, Weakliem and Carter[12] performed a constant pressure MC simulation of the SW potential in the canonical ensemble where the concentrations of Si and Ge were conserved. Due to long correlation times in these simulations, their results on the miscibility gap were not conclusive. More recently, Dünweg and Landau[13] have studied the Keating potential for $Si_{1-x}Ge_x$ alloys by means of an extensive constant pressure, semi-grand-canonical, MC simulation. Their calculations were performed in conjunction with a detailed finite-size scaling analysis allowing them to accurately study the nature of the phase transition. Their most important result was that the phase transition of $Si_{1-x}Ge_x$ alloys has a mean-field-like behavior, unlike most binary alloys. Among their other results was that the linear thermal expansion coefficient is negative at all temperatures, in contradiction to experimental facts.[14] The implication of this result is that the Keating model is not reliable for studying the structural properties of Si or its al-

loys at finite temperature. Hence, a question must be addressed: How much does the choice of the model affect the locus and the nature of the phase transition? In order to answer this question, we have considered an obstensively reliable model for studying the phase behavior of $Si_{1-x}Ge_x$ alloys.

This paper is organized as follows: In Sec. II we present the model, discuss the choice of the parameters, and describe the numerical technique used in our simulations. In Sec. III we present our results, in particular, the phase diagram is presented and the nature of the unmixing critical point is discussed. We also present and discuss, in this section, our results on the structural properties of the binary mixture, including the linear thermal expansion, the dependence of the average bond lengths on the composition of the alloy, and the bond-length and bond-angle distributions. Comparison with previous analytical and numerical calculations will also be considered. Finally, we summarize and conclude in Sec. IV.

II. THE MODEL

In our simulation, we assume that Si and Ge atoms are always located on the nodes of a diamond network with fluctuating bonds and interacting via the Stillinger-Weber potential.[4] This assumption is somewhat midway between a totally continuum-space one and a lattice-gas-like one, although the SW interaction, by itself, is able to produce the diamond network without the prior assumption. Our assumption, however, neglects the presence of vacancies or interstitials in the lattice. Since the concentration of these impurities is vanishingly small in a real system, their total number would be virtually zero within the lattice sizes considered by our simulation, thereby justifying our approximation. This method is very efficient computionally because the nearest-neighbor list is known at the very beginning of the simulation and is used throughout the rest of the computation.

Stillinger and Weber originally proposed their model with a certain parametrization for Si only.[4] Later, Ding and Andersen[8] were able to reparametrize the SW model for Ge and fit their theoretical phonon-dispersion relationship to the experimental one. Fortunately, almost all parameters were found to be identical to those of Si.

Each atom in the system has four degrees of freedom: The first is a discrete variable (or pseudospin) S_i given by the nature of the atom. We choose the notation so that $S_i=+1$ for a Si atom, and $S_i=-1$ for a Ge atom. The three other degrees of freedom correspond to the three coordinates of the atom $\mathbf{r}_i$. The Hamiltonian of the binary mixture can be written as a sum of three terms: A two-body interaction term $\mathcal{H}_2$, a three-body interaction term $\mathcal{H}_3$, and a chemical potential term $\mathcal{H}_1$.

The two-body part of the Hamiltonian can be written as follows:

$$\mathcal{H}_2=\sum_{\langle i,j\rangle}\epsilon(S_i,S_j)F_2[r_{ij}/\sigma(S_i,S_j)]\ , \tag{1}$$

where the sum is performed over all nearest-neighbor bonds $\langle i,j\rangle$. $\epsilon(S_i,S_j)$ corresponds to the covalent binding energies: For Si, $\epsilon(+1,+1)=2.17$ eV and for Ge $\epsilon(-1,-1)=1.93$ eV. For calculating the binding energy between Si and Ge, we adopt the argument of Kelires and Tersoff:[11] Using the Tersoff potential, they derived an unmixing enthalpy $\Delta H=7.3$ meV. Using mean-field considerations, one finds a critical temperature given by $k_BT_c=-[2\epsilon(+1,-1)-\epsilon(+1,+1)-\epsilon(-1,-1)]=2\Delta H$ from which one obtains $\epsilon(+1,-1)=2.0427$ eV. For the ideal bond length of Si we have taken $R_0(+1,+1)=2.34779$ Å, and for Ge we have taken $R_0(-1,-1)=2.445\,98$ Å. Assuming that Végard's law is valid, a mixed system with 50% composition should have a lattice constant which is the arithmetic mean of that of pure Si and pure Ge. Hence we have taken $R_0(+1,-1)=[R_0(+1,+1)+R_0(-1,-1)]/2=2.396\,885$ Å.

The spatial dependence of the two-body interaction is introduced through the function F_c which has the following explicit form:

$$F_2(y)=\begin{cases}A\left[\dfrac{B}{y^p}-\dfrac{1}{y^q}\right]e^{\delta/(y-b)} & \text{for } y<b\\ 0 & \text{for } y\geq b.\end{cases} \tag{2}$$

It is interesting to note that $F_2(y)$ is a function of the rescaled bond length y only, and therefore is the same for both Si and Ge. Another interesting feature of $F_2(y)$ is that, at $y=b$, it vanishes without any discontinuities in its derivatives. The parameters of the function F_2, which are identical for the three types of bonds, are given by[4]

$$A=7.049\,556\,277,\quad B=0.602\,224\,558\,4,\quad p=4,$$
$$q=0,\quad \delta=1,\ \text{and}\ b=1.80\ . \tag{3}$$

At $y=2^{1/6}$, i.e., when $r_{ij}=R_0(S_i,S_j)=2^{1/6}\sigma(S_i,S_j)$, the function F_2 exhibits a minimum equal to -1.

Due to its small coordination number, the diamond structure must be stabilized by an additional three-body interaction, for which we write, generalizing the original SW form,

$$\mathcal{H}_3=\sum_{\langle i,j,k\rangle}[\epsilon(S_i,S_j)\epsilon(S_j,S_k)]^{1/2}\mathcal{L}(S_i,S_j,S_k)\times F_3[r_{ij}/\sigma(S_i,S_j),r_{jk}/\sigma(S_j,S_k)]\times(\cos\theta_{ijk}+\tfrac{1}{3})^2\ , \tag{4}$$

where the sum is performed over all triplets $\langle i,j,k\rangle$ with the vertex at site j (i and k are nearest neighbors of j). The angle between $\mathbf{r}_{ij}$ and $\mathbf{r}_{jk}$ is given by its cosine,

$$\cos\theta_{ijk}=\frac{\mathbf{r}_{ij}\cdot\mathbf{r}_{jk}}{r_{ij}r_{jk}}\ . \tag{5}$$

Here again, the function F_3 depends only on the rescaled bond lengths and is given by

$$F_3(y_1,y_2)=\begin{cases}e^{\gamma/(y_1-b)+\gamma/(y_2-b)} & \text{for } y_1<b \text{ and } y_2<b\\ 0 & \text{otherwise,}\end{cases} \tag{6}$$

where the constant $\gamma=1.20$. The function $\mathcal{L}$ is written as follows:

$$\mathcal{L}(S_i,S_j,S_k)=[\lambda(S_i)\lambda(S_j)^2\lambda(S_k)]^{1/4} \quad (7)$$

with $\lambda(+1)=21.0$ (Ref. 4) and $\lambda(-1)=31.0$.[8] Note that in Eqs. (4) and (7) we have used the geometric mean of the interaction parameters of the pure substances, as has been proposed, e.g., in the paper by Weakliem and Carter.[12]

Finally the chemical potential term is written as

$$\mathcal{H}_1=-\mu_{\mathrm{Si}}\sum_i \delta_{S_i,+1}-\mu_{\mathrm{Ge}}\sum_i \delta_{S_i,-1} , \quad (8)$$

where μ_{Si} and μ_{Ge} are the chemical potentials of Si and Ge, respectively. Since the total number of atoms N is constant, the chemical potential term can then be rewritten, within an additive constant, as

$$\mathcal{H}_1=-\frac{1}{2}(\mu_{\mathrm{Si}}-\mu_{\mathrm{Ge}})\sum_i S_i . \quad (9)$$

The total Hamiltonian of the system is therefore

$$\mathcal{H}=\mathcal{H}_1+\mathcal{H}_2+\mathcal{H}_3 . \quad (10)$$

In our simulation, the pressure remains constant at $P=0$, meaning that the linear sizes of the system in the three directions are allowed to fluctuate independently. This introduces an effective Hamiltonian used in the simulation[13]

$$\mathcal{H}_{\mathrm{eff}}=\mathcal{H}-Nk_BT\ln(\Lambda_x\Lambda_y\Lambda_z) , \quad (11)$$

where Λ_α is the linear size of the system along the direction α.

In Fig. 1, the two-body part of the SW potential is plotted as a function of distance for pure Si. For comparison, we have also plotted on the same graph the two-body part of the Keating model[13] and the Kirkwood model.[15] A clear difference is noticed between the SW potential and the Keating potential: in contrast to the SW potential, the repulsive part of the Keating potential is weaker than its attractive part. As we will see later, this difference is manifested very strongly in the behavior of the linear thermal expansion.

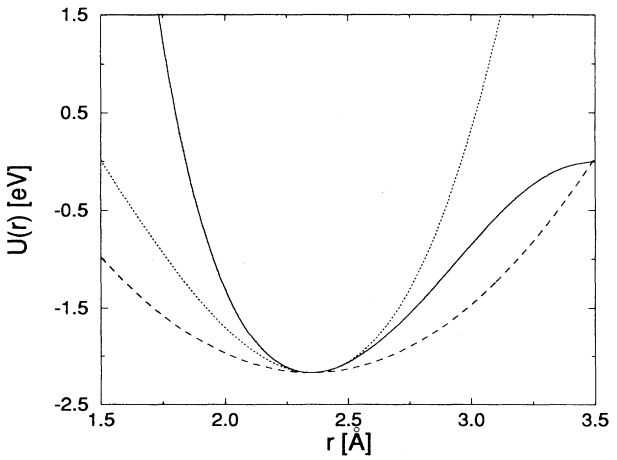

FIG. 1. The two-body parts for pure Si of the Stillinger-Weber potential (solid line), the Keating potential (dotted line), and the Kirkwood model (dashed line) as a function of distance. The minima of the Keating potential and the Kirkwood potential have been adjusted to that of the Stillinger-Weber potential, i.e., at -2.17 eV.

Our MC simulation is performed in the following manner (for more details see Ref. 13): An atom of type S_i at position $\mathbf{r}_i$ is chosen and we then attempt to produce a status S_i' (which might be equal to S_i) at a slightly altered position $\mathbf{r}_i'$. The acceptance or rejection of this attempt is done via the usual Metropolis rejection method using the Hamiltonian in Eq. (10). After each complete sweep over the system, we randomly choose linear sizes for the system Λ_x', Λ_y', and Λ_z' slightly different from the present ones. While the types of the atoms are kept constant, their positions are rescaled by the relative change in the linear system size: $x'=x\Lambda_x'/\Lambda_x$, $y'=y\Lambda_y'/\Lambda_y$, and $z'=z\Lambda_z'/\Lambda_z$; the acceptance or rejection of this attempt is again performed with the Metropolis rejection method using the effective Hamiltonian in Eq. (11). In order to optimize our code, we have divided the network into eight interpenetrating sublattices, so that there are no two-body or three-body interactions between any two atoms on the same sublattice. This allows us to use the checkerboard method, and hence the code is run in a fully vectorized form. Data were obtained using an IBM ES/9000 vector processor. All data presented in Sec. III were calculated very accurately with error bars smaller or comparable to the corresponding symbol size.

III. RESULTS

A. Phase diagram

The equilibrium concentrations of Si and Ge are obtained by sweeping through the chemical potential difference $\Delta=(\mu_{\mathrm{Si}}-\mu_{\mathrm{Ge}})/2$, at fixed temperature; we start deep in the pure Si phase and decrease Δ down to the pure Ge phase before sweeping back up to the pure Si phase. Due to the first-order nature of the phase transition between the Si-rich phase and the Ge-rich phase, hysteresis is observed in x (concentration of Ge) as a function of chemical potential difference. Since on both metastable branches x does not vary very strongly with Δ, we found it sufficient, for our purposes in the present paper, to determine the two coexisting values of x by direct inspection of the hysteresis loops. The resulting phase diagram in concentration-temperature space is shown in Fig. 2, plotted together with the phase diagrams predicted from numerical simulation of the Tersoff model[11] and the Keating model.[13] The accuracy obtained by this simple method is quite satisfactory, and hence we did not try to improve on it. A method which permits the determination of the phase boundaries with even higher accuracy, using thermodynamic integration, has been described in the paper by Dünweg and Landau.[13] However, this method should have needed an increased numerical effort, because it requires the calculation of the difference in the ground-state entropies due to the continuous degrees of freedom.[13]

From Fig. 2, the transition point from the two-phase coexistence region to the disordered phase is estimated

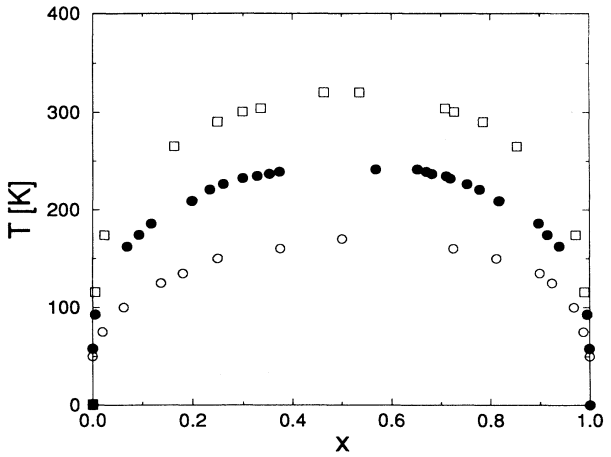

FIG. 2. The phase diagram of a $Si_{1-x}Ge_x$ mixture calculated from the SW model (solid circles), the Tersoff model (open circles), and the Keating model (open squares).

around $k_B T_c = 0.021$ eV, i.e., about 240 K. Using finite-size scaling arguments, a more precise estimation of the transition point is presented in Sec. III B.

Notice that the asymmetry of the model, Eq. (10), is reflected in the shape of the phase diagram. This asymmetry implies that at coexistence there are more Ge atoms in the Si-rich phase than Si atoms in the Ge-rich phase.

It is also of interest to note that the presence of the elastic degrees of freedom has a strong effect on the location of the critical point. In fact, in the absence of the elastic degrees of freedom, the model becomes an Ising model on the diamond lattice, whose transition point is known to be (see Ref. 16) $k_B T_c^{\text{diamond}} = 2.7040\,4J$. With $J = -[2\epsilon(+1,-1) - \epsilon(+1,+1) - \epsilon(-1,-1)]/4$,[13] the transition would be at $k_B T_c = 0.009\,87$ eV which is roughly half that found in our simulation. Although using a different model, the simulation of the Keating model[13] also finds that the elastic effects roughly double the critical temperature yielding T_c about 320 K. We should also note that our estimate for the critical temperature is larger than that calculated by Kelires and Tersoff,[11] and by the *ab initio*–based MC simulation of de Gironcoli, Giannozzi, and Baroni.[17] Both find roughly $T_c \approx 170$ K.

B. Critical behavior

In this subsection we turn to the discussion of the nature of the phase transition from the two-phase coexistence to the disordered, mixed phase. The numerical study using the Keating model found critical behavior belonging to the mean-field universality class.[13] It has been argued that although it includes elastic interactions, the Keating model for $Si_{1-x}Ge_x$ is different from the compressible Ising model which has been shown to exhibit a weak first-order phase transition using a renormalization-group calculation.[18] Their argument is based on the fact that the Keating Hamiltonian is not invariant under an exchange between Si and Ge (and a simultaneous $\Delta \rightarrow -\Delta$ change), and/or the fact that the simulation is effectively run with infinite shear modulus. Both properties are retained in the present model, and hence one can expect similar behavior as for the Keating model, i.e., mean-field-like behavior, due to the elastic interactions between the atoms which result in an effective long-range spin-spin interaction.

A thorough numerical investigation of the nature of a phase transition can be performed only through finite-size scaling analysis.[19] In order to provide conclusive results, we have adopted the multihistogram reweighting method whose description can be found in Refs. 13 and 20. We briefly describe the method and refer the reader to Ref. 13 for more details. We rewrite the Hamiltonian in Eq. (10) as follows:

$$\mathcal{H} = \mathcal{U} - \Delta M \ , \tag{12}$$

where $\mathcal{U}$ is the "core" internal energy and M is defined as

$$M = \sum_{i=1}^{N} S_i \ . \tag{13}$$

For a given system size, two-dimensional histograms are then obtained as a function of $\mathcal{U}$ and M for several values of temperature and chemical potential difference Δ. We then solve the multihistogram equations using the Aitken acceleration method.[13]

Four system sizes, $N = 512$, 2744, 4096, and 8000, were simulated at multiple values of $(\Delta, k_B T)$ near the estimated phase transition. In order to obtain very good statistics all simulations were run over 10^6 MCS.

Physical quantities which are interesting for the analysis of the critical behavior are: M, its corresponding susceptibility

$$\chi = \frac{1}{N k_B T}(\langle M^2 \rangle - \langle M \rangle^2) \tag{14}$$

and its related fourth-order cumulant defined as

$$U_4 = 1 - \frac{\langle (M - \langle M \rangle)^4 \rangle}{3\langle (M - \langle M \rangle)^2 \rangle^2} \tag{15}$$

which has been proven to be extremely sensitive to the nature of the phase transition.[19,21] At constant temperature, the fourth-order cumulant, for an infinite system, exhibits as a function of Δ a maximum equal to $\frac{2}{3}$ at the first-order transition line. At the critical point, the fourth-order cumulant is discontinuous, and has a nontrivial value which depends solely on the universality class. For temperatures larger than the critical point, the fourth-order cumulant is identically zero. For finite system sizes, however, $U_4(T)$ is regular at all temperatures, and the discontinuity found in the thermodynamic limit is rounded. However, cumulants for different system sizes cross at the nontrivial fixed-point value. The maximum of the fourth-order cumulant (along the coexistence line between Si and Ge) is displayed in Fig. 3, in the vicinity of the critical point. The cumulants for the various system sizes cross at $U_4^* \approx 0.28$ which is very close to the mean-field fixed point $U_4^{mf} \approx 0.2705\,2$ (Ref. 22) and very different from that of the three-dimensional Ising model, $U_4^{\text{Ising}} \approx 0.47$.[23] Our results, therefore, rule out the possibility that the critical behavior of the system

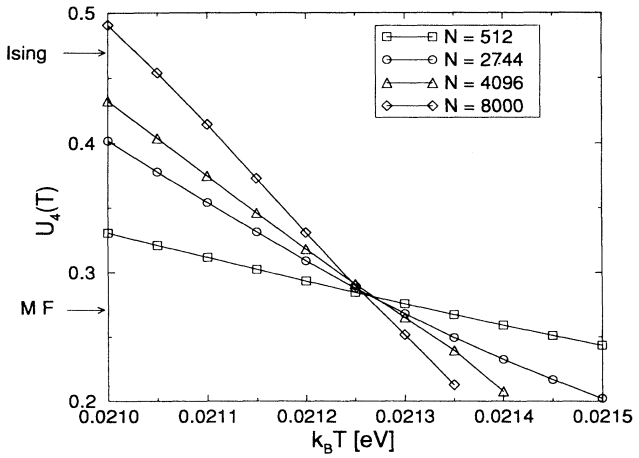

FIG. 3. Fourth-order cumulant $U_4(T)$ as a function of temperature plotted for all system sizes.

is in the same universality class as the three-dimensional Ising model. The transition cannot be first order since for a two-state model, such as ours, $U_4^{\text{f.o.}}=0.5$.[24] From the crossing of the fourth-order cumulants, the transition temperature is estimated more precisely at about 247 K.

Physical quantities, in the vicinity of a second-order phase transition, exhibit an extremely interesting finite-size scaling behavior for temperatures or chemical potentials at which the finite system size is smaller than the correlation length which diverges at the critical point. However, the finite-size scaling laws are very different for systems for which hyperscaling is valid and for those for which it is not. The hyperscaling relation reads $d\nu=2-\alpha$, where d is the dimensionality of the system and ν and α the critical exponents of correlation length and specific heat, respectively. A mean-field system ($\alpha=0,\nu=\frac{1}{2}$) does, in general, not obey this relation (except in four spatial dimensions), while it is valid for the universality class of the three-dimensional Ising model ($\alpha\approx 0.12,\nu\approx 0.63$ (Ref. 23)).

For systems for which hyperscaling is valid, the following finite-size scaling relations, among others, hold in the vicinity of the critical point: The susceptibility scales with the linear system size L as[19]

$$\chi(T)=L^{\gamma/\nu}\tilde{\chi}(tL^{1/\nu}) \tag{16}$$

and the fourth-order cumulant as

$$U_4(T)=\tilde{U}(tL^{1/\nu}) . \tag{17}$$

In Eqs. (16) and (17), t is the reduced temperature, $t=|1-T/T_c|$, while γ is the critical exponent for the susceptibility ($\gamma\approx 1.24$ in the universality class of the three-dimensional Ising model;[23] all critical exponents refer to the corresponding infinite system size).

On the other hand, for a mean-field system the total number of sites L^d is the relevant quantity. Hence in this case the relations read[22]

$$\chi(T)=L^{d/2}\tilde{\chi}(tL^{d/2}) \tag{18}$$

and

$$U_4(T)=\tilde{U}(tL^{d/2}) . \tag{19}$$

We found excellent mean-field-like scaling of the fourth-order cumulant, as shown in Fig. 4(a). For comparison, we also tried Ising-like behavior [Eq. (17)] and found fairly good scaling as well, although poorer than for the mean-field case. The nature of the universality class is usually better detected through the exponent γ. In Fig. 4(b), we have plotted the susceptibility scaling function $\tilde{\chi}$ using the mean-field scaling relation Eq. (18) from which we observe a very nice data collapsing. When we used Eq. (16) with the exponents of the three-dimensional Ising model, the scaling was fairly poor. This also implies that the critical behavior must belong to the mean-field universality class.

C. Lattice properties

Based on simulations of a 512-atom system we have calculated the lattice constant as a function of temperature for both pure Si and pure Ge. In Fig. 5, the lattice constant for pure Si is plotted together with the experi-

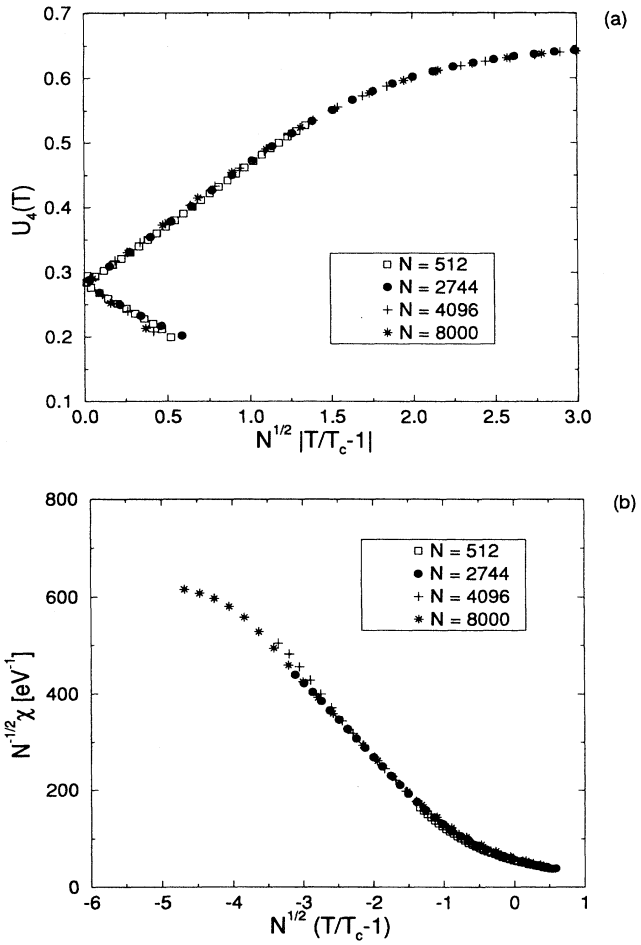

FIG. 4. (a) Fourth-order cumulant versus absolute value of scaled temperature [cf. Eq. (19)]. (b) Scaled susceptibility versus scaled temperature [cf. Eq. (18)]. In both figures, mean-field scaling is used.

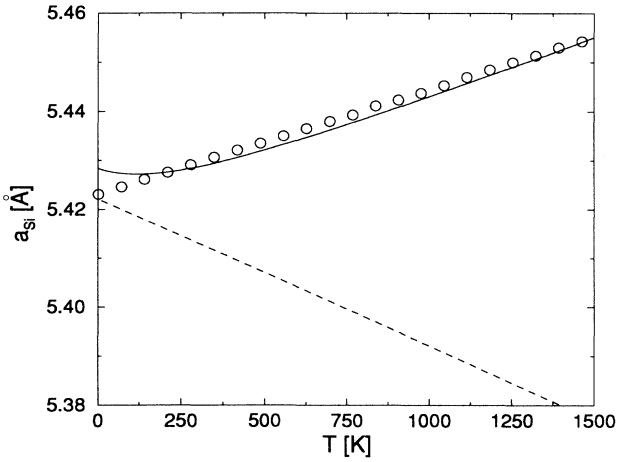

FIG. 5. Lattice constant of pure Si as a function of temperature. The circles are from the MC simulation of the SW model, the solid line is a fit to experimental data (see Ref. 14, pp. 15 and 16), and the dashed line is from the MC simulation of the Keating model (see Ref. 13).

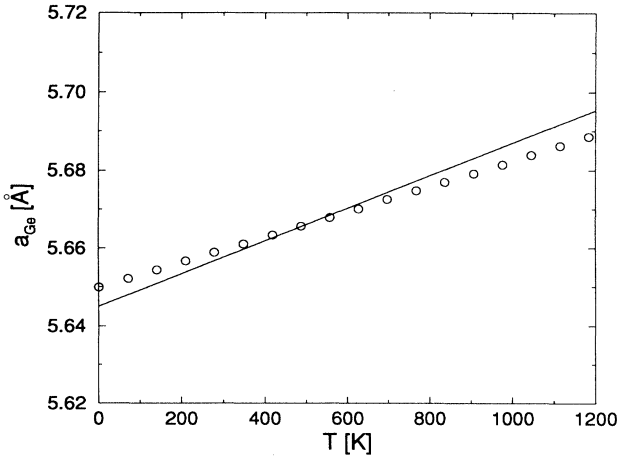

FIG. 6. Lattice constant of pure Ge as a function of temperature. The circles are from the Monte Carlo simulation of the SW model, and the solid line is a fit to experimental data (see Ref. 14, pp. 31 and 32).

mental results.[14] We note that for pure Si, our MC results are largely in agreement with the experimental data, an observation which gives further testimony for the reliability of the SW model. However, we must note that experiments find a negative linear thermal expansion at low temperatures ($T \leq 120$ K) in contradiction with our results. This discrepancy implies that the SW model is not very reliable at very low temperatures. It is, however, conceivable that the SW model with correctly quantized phonons might yield correct behavior.[25] For comparison, in Fig. 5 we have also shown the lattice constant as obtained from MC simulation of the Keating model.[13] These latter data show completely unphysical behavior, i.e., a negative thermal expansion at all temperatures. We believe that this can be qualitatively understood from the fact that the two-body part of the Keating potential is flatter for distances smaller than the minimum position and steeper for larger distances (see Fig. 1). Consequently a large bond length has a much larger energy penalty than a smaller one. Therefore, thermal excitations tend to decrease the average bond length. This effect more than compensates for the increase in translational entropy when the volume increases.

For pure Ge, as shown in Fig. 6, the comparison between our MC prediction and the experimental data, although fairly good, is poorer than for Si. We believe that an improvement of this comparison can be achieved by a reparametrization of the SW potential for Ge.[8,26]

The local structure of the binary alloy in the disordered phase can be investigated through the mean Si-Si, Ge-Ge, and Si-Ge bond lengths. In Fig. 7, where the three bond lengths are displayed as a function of Ge composition, we observe that the bonds relax linearly and with the same rate as x is increased. The same trend was observed through previous calculations.[15,17,27]

The average lattice constant is related linearly to the average bond length through $a_{Si_{1-x}Ge_x} = 4l_x/\sqrt{3}$, where l_x is the average bond length at composition x. Therefore, the results in Fig. 7 imply that the average lattice constant depends linearly on x, in agreement with Végard's law.[12–17,27–30] In Fig. 7, we have also plotted the average bond length obtained from the MC simulation of the Keating model.[13] The fact that the Keating model predicts an average bond length slightly lower than that obtained from the SW model is due to the negative linear thermal expansion in the Keating model.

Around their mean values, the three types of bonds exhibit fluctuations as shown by the bond-length distributions in Fig. 8 for almost equal concentrations of Ge and Si and at $k_B T = 0.025$ eV. The distributions are normal-

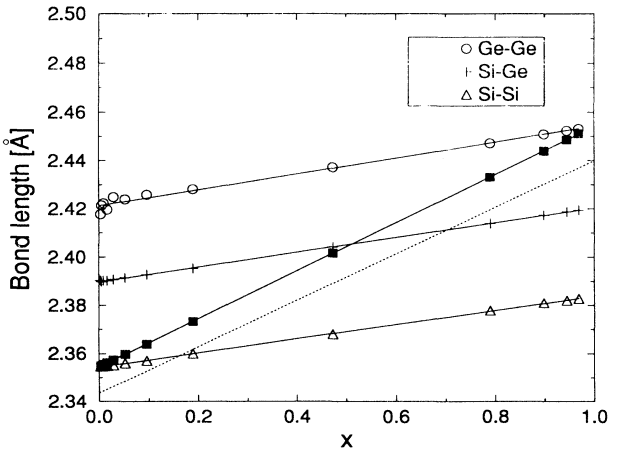

FIG. 7. Mean nearest-neighbor bond lengths as a function of Ge concentration calculated at $k_B T = 0.03$ eV. Solid squares correspond to the mean nearest-neighbor bond length and solid lines are linear fits to the numerical data. The dashed line is from the MC simulation of the Keating model at $k_B T = 0.05$ eV (Ref. 13).

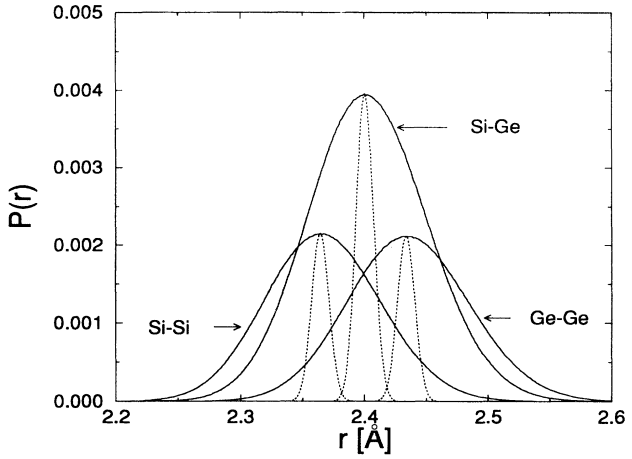

FIG. 8. Bond-length distributions calculated at $k_B T=0.025$ eV and $\Delta=0.479\,51$ eV. At these conditions, $x\approx 0.505$. The dotted lines correspond to the analytical calculation of Mousseau and Thorpe (Ref. 15). Their distributions are normalized in such a way that their heights are equal to ours.

ized so that the sum of the areas under the three distributions equals unity. We first notice that all three distributions are very close to Gaussian with a slight asymmetry. In fact, we observed that the right branch of each distribution (i.e., for distances larger than the position of the peak) is slightly wider than the left branch, but each branch can be very well described by a Gaussian. This asymmetry is again associated with the fact that the shape of the two-body part of the SW potential is flatter for distances larger than the minimum position than for smaller distances.

In Fig. 8, we have also shown the distributions calculated analytically by Mousseau and Thorpe[15] (dotted lines). The large discrepancy between our numerical data and their theoretical prediction arises from the fact that they have performed their calculations at $T=0$, whereas our calculations take into account thermal fluctuations making the distributions wider. In order to show that the width of our distributions results from thermal fluctuations, we have considered an artificial situation where Si and Ge are mixed at low temperatures. This was done by randomly distributing Si and Ge atoms on the diamond network, and disallowing type flips, while equilibrating

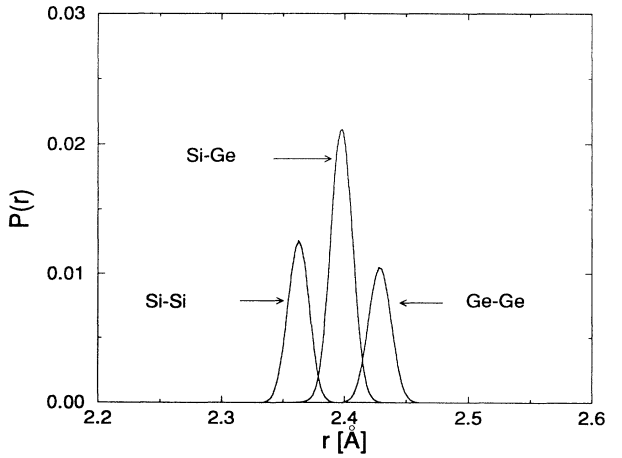

FIG. 9. Bond-length distributions calculated at $k_B T=0.0005$ eV and $x=0.4863$.

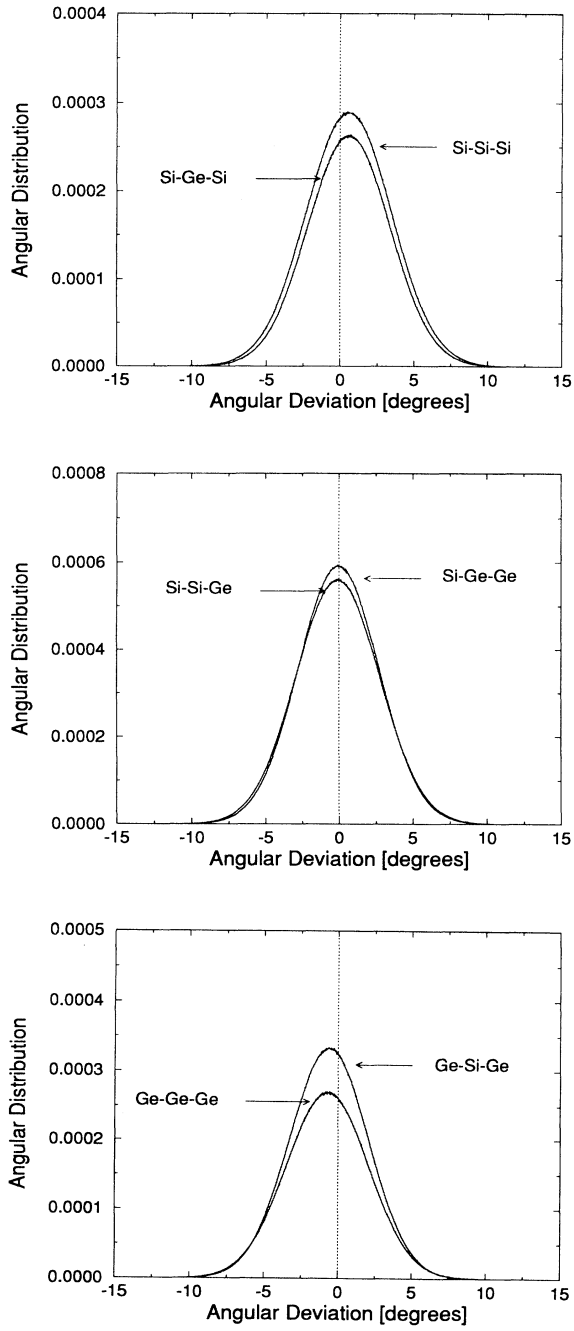

FIG. 10. Bond-angle distributions for the same conditions as Fig. 8. The vertical dotted lines indicate the location of the origin.

the translational degrees of freedom at $k_BT=0.0005$ eV. At such a low temperature the distributions, shown in Fig. 9, are very narrow, and very close to those calculated in Ref. 15, due to the lack of thermal fluctuations. We should note, however, that the configurations from which we have calculated these distributions are not stable since Si and Ge totally unmix at such a low temperature.

Like the bond lengths, the bond angles also exhibit deviations from their ideal value $\theta_{\text{ideal}}=109.4712°$. We have separated the distributions into three groups: Angles with two Si ends as shown in Fig. 10(a); those with one end being a Si and the other being a Ge shown in Fig. 10(b); and finally those with two Ge ends shown in Fig. 10(c). These distributions are calculated for the particular case where the Si and Ge concentrations are essentially equal. Unlike the bond-length distributions, the bond-angle distributions are completely symmetric and very well fitted by a Gaussian. We observe that the average deviation of the bond-angle value (corresponding to the maximum of each distribution) is positive when the two ends of the angle correspond to Si atoms [see Fig. 10(a)], that the maximum position is at zero when one end is occupied by a Si and the other one by a Ge [Fig. 10(b)], and that the maximum position is negative when the two ends are occupied by Ge atoms [Fig. 10(c)]. A similar behavior has already been observed through the numerical simulation of Weidmann and Newman.[27] This trend of the bond-angle distribution can be understood using the following arguments: For a Si-Si-Si angle, statistically speaking, at least one of the two other atoms connected to the central atom will be a Ge atom, which will push the central Si atom leading to the broadening of the angle. Using the same argument, we can explain why angles with two Ge atoms at the end are on average smaller than the ideal angle. For a mixture with $x=0.5$, an atom surrounded by two Si atoms and two Ge atoms does not have any preferred direction for symmetry reasons, implying that the average bond angle for the two following angles Ge-Si-Si and Ge-Ge-Si must be ideal.

IV. CONCLUSION

The behavior of $Si_{1-x}Ge_x$ alloys has been investigated in detail by means of Metropolis Monte Carlo simulations of the SW model. The simulations were performed at constant pressure in the semi-grand-canonical ensemble. The phase diagram of the binary system exhibits a low-temperature coexistence region followed by a homogeneous disordered phase at high temperatures. Due to the difference in the atomic sizes of Si and Ge, the phase diagram is slightly asymmetric. The first-order line separating Si- and Ge-rich phases is terminated by a critical point estimated quite accurately at 247 K. A detailed finite-size scaling study of the critical point, combined with the multihistogram reweighting method, shows unambiguously that the critical point exhibits mean-field-like critical behavior, presumably due to an effective long-range interaction resulting from the elastic interactions between the atoms.

We have also studied the structural properties of the constituent elements of the binary alloy. In particular, we have calculated the lattice constants for pure Si and pure Ge as a function of temperature, and found very good agreement with experiments. For Si, experiments have shown that the linear thermal expansion coefficient is negative for temperatures below 120 K, whereas in the SW model it is always positive.

Above the critical point, the average lattice constant is found to comply with Végard's law, i.e., the lattice constant of the mixture depends linearly on the Ge composition. We also found that this law is practically independent of temperature due to the very small linear thermal expansions of both of Si and Ge.

The structural behavior of the mixed alloy is also investigated through the bond-length and bond-angle distributions. We found that the bond-length distributions are very close to Gaussian, in agreement with the calculations of Mousseau and Thorpe.[15] However, unlike their analytical prediction and a related simulation,[27] the distributions calculated in the present work are wider due to the inclusion of thermal fluctuations in the MC simulation. The bond-angle distributions were also found to have a Gaussian shape, but they are also wider than those found in previous simulations, due again to thermal fluctuations. To our knowledge, there are no experimental results to compare with.

ACKNOWLEDGMENTS

We wish to thank M. F. Thorpe for helpful comments and discussions. This work was supported in part by the IBM corporation and by NSF Grant No. ASC-9211130.

[1]S. C. Jain, J. R. Willis, and R. Bullogh, Adv. Phys. **39**, 127 (1990).
[2]J. G. Kirkwood, J. Chem. Phys. **7**, 506 (1939).
[3]P. N. Keating, Phys. Rev. **145**, 637 (1966).
[4]F. H. Stillinger and T. A. Weber, Phys. Rev. B **31**, 5262 (1985).
[5]R. Biswas and D. R. Hamman, Phys. Rev. Lett. **55**, 2001 (1985).
[6]J. Tersoff, Phys. Rev. Lett. **56**, 632 (1986).
[7]E. R. Cowley, Phys. Rev. Lett. **60**, 2379 (1988).
[8]K. Ding and H. C. Andersen, Phys. Rev. B **34**, 6987 (1986).
[9]I. P. Batra, F. F. Abraham, and S. Ciraci, Phys. Rev. B **35**, 9552 (1987).
[10]In this paper, we prefer to use the phrase "semi-grand-canonical ensemble" instead of "grand-canonical ensemble" since in contrast to the usual grand-canonical ensemble, the total number of particles is kept constant in our study while the difference in the total numbers of atoms of the two species is allowed to fluctuate.
[11]P. C. Kelires and J. Tersoff, Phys. Rev. Lett. **63**, 1164 (1989).
[12]P. C. Weakliem and E. A. Carter, Phys. Rev. B **45**, 13 458 (1992).
[13]B. Dünweg and D. P. Landau, Phys. Rev. B **48**, 14 182 (1993).
[14]*Semiconductors, Group IV Elements and III-V Compounds*, edited by O. Madelung (Springer-Verlag, Berlin, 1991).

[15]N. Mousseau and M. F. Thorpe, Phys. Rev. B **46**, 15 887 (1992).
[16]M. E. Fisher, Rep. Prog. Phys. **30**, 615 (1967).
[17]S. de Gironcoli, P. Giannozzi, and S. Baroni, Phys. Rev. Lett. **66**, 2116 (1991).
[18]D. J. Bergmann and B. I. Halperin, Phys. Rev. B **13**, 2145 (1976).
[19]*Finite Size Scaling and Numerical Simulation of Statistical Systems,* edited by V. Privman (World Scientific, Singapore, 1990).
[20]A. M. Ferrenberg and R. H. Swendsen, Phys. Rev. Lett. **63**, 1195 (1989).
[21]K. Binder and D. P. Landau, Phys. Rev. B **30**, 1477 (1984).
[22]E. Brezin and J. Zinn-Justin, Nucl. Phys. B **257**, 867 (1985).
[23]A. M. Ferrenberg and D. P. Landau, Phys. Rev. B **44**, 5081 (1991).
[24]K. Binder, K. Vollmayr, H.-P. Deutsch, J. D. Reger, M. Scheucher, and D. P. Landau, Int. J. Mod. Phys. C **3**, 253 (1992).
[25]The thermal expansion of Si in the low-temperature regime is well understood: see C. H. Xu, C. Z. Wang, C. T. Chan, and K. M. Ho, Phys. Rev. B **43**, 5024 (1991).
[26]Z. Jian, Z. Kaiming, and X. Xide, Phys. Rev. B **41**, 12 915 (1990).
[27]M. R. Weidmann and K. E. Newman, Phys. Rev. B **45**, 8388 (1992).
[28]L. Végard, Z. Phys. **5**, 17 (1921).
[29]R. A. Logan, J. M. Rowell, and F. A. Trumbore, Phys. Rev. **136**, A1751 (1964).
[30]M. Matsuura, J. M. Tonnerre, and G. S. Gargill III, Phys. Rev. B **44**, 3842 (1991).
[31]Y. Cai and M. F. Thorpe, Phys. Rev. B **46**, 15 872 (1992); **46**, 15 879 (1992).